

ANALYSIS OF CAMERA SYSTEMATIC ERRORS IN AN ADS40 DATASET

V. Casella^a, M. Franzini^a

^aDIET, University of Pavia, Via Ferrata, 34 - I - 27100 Pavia, Italy
(vittorio.casella, marica.franzini)@unipv.it

Commision I, WG I/4

KEY WORDS: Photogrammetry, Calibration, Digital Camera

ABSTRACT

The paper concerns an ADS40 dataset acquired in August 2004 by the Italian company Compagnia Generale Ripresearee (CGR) over the Pavia test-site, located in northern Italy. The dataset is composed of three blocks characterized by the flying heights 2000 m, 4000 m and 6000 m.

Camera systematic errors are focused in a three-fold way. Single model errors are assessed first for the 2000m block: instead of the usual procedure of performing multiple forward intersection of check points, single-model, two-ray combinations are considered, along-track and across-track. Second, camera self-calibration is performed at the three considered flying heights and the so obtained calibrations are compared between themselves and with the old one. Finally, the new calibrations are assumed and the 2000 m block is assessed again, in order to quantify the accuracy gain.

1. INTRODUCTION

1.1 Background

The photogrammetric processing of imagery produced by airborne line cameras is a challenging research area. The complete definition of topics like camera models, trajectory models, camera calibration still need investigations and case studies.

The dataset considered in the paper has already been analyzed within several papers. Some of them report activities wholly developed at the University of Pavia (Casella et al., 2007, 2nd and 3rd items) while others concern joint activities carried out at the University of Pavia and at the IGP, ETH Zurich (Casella et al., 2007, 1st reference; Kocaman et al., 2007; 1st and 2nd reference). Joint papers are based on the use of exactly the same dataset (in terms of image coordinates, weights of observations, the distinction between control and check points, their object coordinates) and of different orientation algorithms and programs. At the University of Pavia, the commercial Socet-Set, Orima and GPro programs were used, delivered by the Leica Geosystems company (Sandau et al., 2000; Hinsken et al., 2002; Tempelmann et al., 2003). At the IGP, ETH, algorithms and programs developed within the Institute were used (Gruen and Zhang, 2003; Kocaman et al., 2006). Interestingly, results of the two Groups are equivalent and show, for all the three blocks, the same phenomena and behaviours: very briefly, there are strong biases in the object coordinates of check points in Direct Georeferencing (DG); it is impossible to reach sub-pixel accuracy with mere aerial triangulation; when camera self-calibration is performed, accuracy is increased to small fractions (1/4 to 1/6) of the pixel. Further details can be found in the quoted papers and partially in Section 3.

Other experiences concerning the ADS40 camera are based on a dataset acquired over the Vaihingen, Stuttgart, test site. Cramer (2006) and Kocaman et al. (2006) confirm that self-calibration is necessary to obtain top-quality accuracies.

1.2 Goal and structure of the paper

Almost all the available literature on ADS40 emphasizes the necessity of camera self-calibration: this highlights the presence of camera systematic errors and implies that the internal camera geometry changes with time.

Nevertheless, to the authors' knowledge, no paper concerns in-depth analysis of these errors, so that several questions still remain open, questions like: what is the size of camera systematic errors? What is the contribution of these biases to the error budget in DG mode? Is there a time span over which the internal camera geometry is reasonably stable?

The present paper concerns the above listed questions and has three main topics.

1. Errors of single-model photogrammetric measurements are assessed for the 2000 m block: instead of the usual procedure of performing multiple forward intersection of check points, single-model, two-ray combinations are considered, along-track and across-track.
2. Camera self-calibration is performed at the three considered flying heights and the newly obtained calibrations are compared between themselves and with the original one, supplied by the company which performed the flights.
3. The new calibrations are assumed and the 2000 m block is assessed again, in order to quantify the accuracy gain.

Section 2 illustrates the dataset used, while *Section 3* summarizes main test results for the 2000 m block, illustrated in previous papers. *Section 4* deals with the assessment of the 2000 m block in terms of single-model measurements. In *Section 5* three new calibrations are obtained for the three blocks 2000, 4000 and 6000 m. In *Section 6* the new calibrations are adopted and the 2000 m block is assessed again. Finally, *Section 7* synthesizes the conclusions of the paper.

2. THE DATASET

In August 2004 three ADS40 photogrammetric blocks were acquired over the Pavia Test Site (PTS) by the Italian company

Compagnia Generale Ripresearee (CGR), characterized by the flying heights 2000 m, 4000 m and 6000 m; their GSD values are 20, 40 and 60 cm, respectively.

In the present paper the 2000 m block is mainly focused on, whose structure is shown in Figure 1, together with the position of the 50 control points available, having a size of 60 cm. Only one GCP configuration is considered in the paper, constituted by 12 points: the four red corner points plus the green ones; all the other dots represent check points. The blue rectangle represents the area where the triangulation is performed, while the three labels indicate strip names.

CGR also provided the authors with camera calibration, constituted by the so-named CAM files, and the three misalignment angles between IMU and camera. Calibration was performed by Leica Geosystems and the corresponding certificate was issued on 1.3.2004.

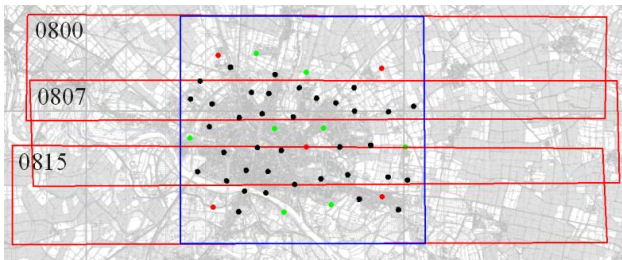


Figure 1. Structure of the 2000 m block and distribution of control points

3. FROM PREVIOUS PAPERS: ASSESSMENT OF THE 2000 M BLOCK

Three scenarios are considered:

- **DG**, in which the exterior orientation parameters (EOPs) measured by the GPS/IMU are used directly;
- **BASIC**, where aerial triangulation is performed and EOPs coming from the GPS/IMU are inserted into the adjustment as observations, together with tie points and GCPs;
- **SELF**, in which camera self-calibration is performed, plus a datum transformation is estimated and the misalignments between camera and IMU are re-determined.

Set	GCPs/ CKPs	Comp.	Mean [m]	STD [m]	RMSE [m]
DG	0 / 46	x	0.015	0.119	0.120
		y	-0.007	0.093	0.093
		z	-0.558	0.319	0.643
BASIC	12 / 34	x	0.043	0.212	0.217
		y	-0.011	0.215	0.215
		z	-0.258	0.114	0.282
SELF	12 / 34	x	-0.009	0.055	0.056
		y	-0.010	0.036	0.037
		z	-0.008	0.062	0.062

Table 1. Assessment of the 2000 m flight in terms of multiple forward intersection

For the BASIC and SELF configurations, 12 GCPs are used. A detailed illustration of the measurements performed on the imagery and of the weights used in the adjustments can be found in Casella et al. (2007, the 1st reference).

In all the scenarios, object coordinates of check points (CKPs) are determined through multiple forward intersection and compared to the true ones. Forward intersection is performed by means of a Matlab program developed at the University of Pavia. Results are summarized in Table 1 and show that **DG** presents a strong bias in Z; in previous discussions with other

researchers and experts, GPS was often indicated as the most probable cause of this bias; also, X and Y components appear to be unbiased, but the next Sections will show that the situation is more complex. The BASIC configuration has RMSE values all above the pixel size; the SELF mode shows very good results and RMSEs are all below 1/3 of the pixel. Detailed comments can be found in the quoted literature.

By comparison with figures shown in Section 4, it happens that the measurements assessed in Table 1, being determined by multiple rays, tend to hide some interesting phenomena, which are instead revealed when single-model analysis is performed.

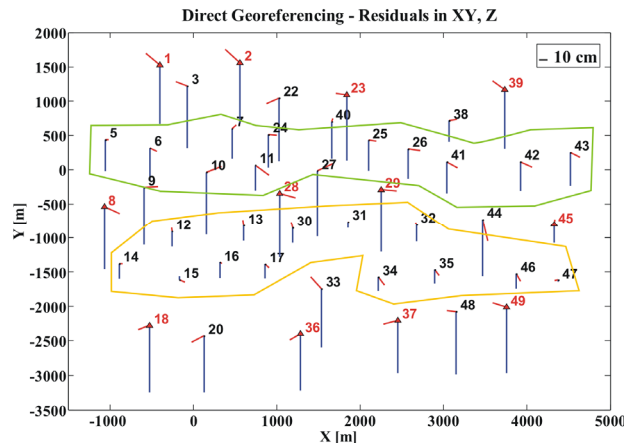


Figure 2. Object space residuals of check point coordinates obtained from DG

Plots of object coordinate residuals are interesting too. Figure 2 concerns the DG scenario: blue vertical lines show height residuals while red lines refer to the planimetric ones. The Z bias is clearly visible and five regions can be identified: those enclosed within the green and yellow polygons and the other three which are above, between and below the polygons. In the last three regions, Z residuals present a comparable bias; in the green region the bias size is decreased and in the yellow polygon is reduced again. The next Section will clarify the origin of this behaviour.

4. SINGLE-MODEL MEASUREMENTS IN THE DG SCENARIO FOR THE 2000 M BLOCK

Table 1 is determined through multiple forward intersection, in which each CKP is determined by all its homologous rays. In the present section single-model measurements are considered instead, in which one point is determined by the intersection of two rays. They are performed in the DG scenario only.

When single-model measurements are considered, many combinations are allowed. Within a single strip there are three images, acquired along the backward, nadir and forward directions, therefore three along-track models can be formed: nadir-backward (NB), nadir-forward (NF) and backward-forward (BF). When two adjacent strips are considered, 9 across-track models can be formed, in line of principle.

Prior to execution of the experiments described in the paper, a detailed simulation work was performed. The nominal three-line camera model was adopted, which can be summarized as follows. An image coordinate system is defined on the focal plane of the camera: the origin coincides with the principal point, the x-axis is parallel to the flight direction, and y-axis is parallel to the sensor lines. Sensor lines occupy the nominal positions; they are assumed to be straight and planar. The CCD elements are equally spaced and the lens is undistorted.

The simulation is based on the following workflow: (i) the true object coordinates of a number of check points are established, as well as the true image coordinates of their projections onto the backward, nadir and forward images of two adjacent strips; (ii) systematic errors are introduced by changing the image coordinates, corresponding to the most common deviations of camera geometry from the nominal model: offset, scale and rotations of CCD lines; (iii) object coordinates of check points are determined by forward intersection and compared with the true ones. Simulation results aren't reported here for space reasons, but they highlight that the various bias sources affect in a variable way the different stereoscopic models.

Therefore single-model measurements are adopted in order to assess single error sources. For each check point considered, a Matlab program, specifically developed, looks for all the stereoscopic models in which that point is visible; the point is stereoplotted in each possible model; residuals are calculated between the measured coordinates and the true ones; a file containing all the determinations of all the available CKPs is created. Other software tools allow the user to filter results in order to analyze specific subsets of the performed measurements.

4.1 Along-track models within a single strip

Primarily, the different behaviours are investigated of the three models NB, NF and BF which can be formed within a single strip. Results are similar for all the three strips and Table 2 concerns strip 0807.

Models	N. CKPs	N. Obs.	Comp.	Min [m]	Max [m]	Mean [m]	STD [m]	RMSE [m]
NB	32	32	x	0.050	0.515	0.182	0.081	0.199
			y	-0.709	0.688	-0.008	0.380	0.380
			z	-1.185	-0.136	-0.822	0.263	0.863
NF	31	31	x	0.051	0.304	0.172	0.054	0.180
			y	-0.679	0.401	-0.094	0.325	0.338
			z	-1.165	-0.531	-0.894	0.123	0.902
BF	31	31	x	0.048	0.303	0.182	0.058	0.191
			y	-0.672	0.505	-0.028	0.350	0.352
			z	-1.147	-0.547	-0.876	0.119	0.884

Table 2. Accuracy for along-track models of the 0807 strip

Regarding systematic errors (see the *Mean* column), results are almost identical for the X and Z components in the three models, while the Y component shows limited variations. Concerning random errors (see the *STD* column) there are significant variations of the Z component which are probably due to the different base-to-height ratios of the three considered models.

4.2 Along-track and across-track models compared

Figures considered in Section 4.1 can be summarized by averaging results for all the along-track models of a strip.

Strip	N. CKPs	N. Obs.	Comp.	Min [m]	Max [m]	Mean [m]	STD [m]	RMSE [m]
0800	18	52	x	-0.190	0.154	-0.041	0.109	0.117
			y	-0.699	0.259	-0.225	0.266	0.348
			z	-1.225	-0.635	-0.913	0.127	0.922
0807	32	94	x	0.048	0.515	0.179	0.065	0.190
			y	-0.709	0.688	-0.043	0.351	0.354
			z	-1.185	-0.136	-0.863	0.183	0.883
0815	21	61	x	-0.439	-0.092	-0.159	0.053	0.168
			y	-0.171	0.800	0.264	0.249	0.363
			z	-1.141	-0.382	-0.827	0.146	0.839

Table 3. Accuracy of the along-track models of the three strips

Table 3 reports assessment results for the three considered strips. They present varying and significant X and Y biases (greater than those shown in Figure 1), while the Z systematic component is almost constant and around -0.86 m, much greater in size than in Table 1. The origin of the Y bias will be further analyzed in the following; the X systematic errors are probably due to IMU misalignments, but the development of this topic is beyond the scope of the present paper. Regarding random components, the Y standard deviation values are much greater than the X ones, because of a systematic pattern of Y residuals, shown in Figure 3.

Table 4 shows results for across-track models, which can be considered only for points which are in the overlapping region of two strips. The table separately analyzes the area between strips 0800 and 0807, corresponding to the green polygon in Figure 2, and the region between strips 0807 and 0815, marked in yellow.

Strip	N. CKPs	N. Obs.	Comp.	Min [m]	Max [m]	Mean [m]	STD [m]	RMSE [m]
0800 0807	12	105	x	-0.240	0.518	0.106	0.163	0.194
			y	-0.236	0.242	-0.026	0.112	0.115
			z	-0.988	0.213	-0.247	0.331	0.413
0807 0815	14	114	x	-0.345	0.367	0.025	0.174	0.175
			y	-0.184	0.165	-0.010	0.066	0.067
			z	-0.729	0.590	0.030	0.345	0.347

Table 4. Accuracy for the across-track models: the combinations 0800-0807 and 0807-0815 are treated separately

Table 4 shows that the subset 0800-0807 has a Z bias of -0.25 m while the subset 0807-0815 has 0.03 m. Across-track models behave very differently than along-track models, concerning Z systematic errors, and this explains Figure 2. Points outside the polygons are only visible in along-track models and their Z residuals are around -0.86 m; inside points are determined with the contribution of along-track and across-track models so their Z residuals come from the averaging of figures shown in Table 3 and Table 4.

4.3 Overall accuracy

Table 5 synthesizes previous results and shows results for three subsets: **All**, indicating all the determinations of the CKPs; **Along**, concerning all the measurements performed in along-track models; **Across**, regarding across-track models only.

Models	N. CKPs	N. Obs.	Comp.	Min [m]	Max [m]	Mean [m]	STD [m]	RMSE [m]
All	46	426	x	-0.439	0.518	0.044	0.171	0.176
			y	-0.709	0.800	-0.008	0.255	0.255
			z	-1.225	0.590	-0.473	0.476	0.671
Along	46	207	x	-0.439	0.515	0.024	0.166	0.168
			y	-0.709	0.800	0.002	0.354	0.354
			z	-1.225	-0.136	-0.865	0.162	0.880
Across	26	219	x	-0.345	0.518	0.064	0.173	0.184
			y	-0.236	0.242	-0.018	0.091	0.093
			z	-0.988	0.590	-0.103	0.365	0.379

Table 5. Overall accuracy assessment for the whole block

4.4 Further analysis on the Y component

As highlighted in previous Sections, the Y component presents high standard deviation values in along-track models, see for instance Table 3. Figure 3 shows residuals for the along-track measurements in the 0807 strip. Blue lines represent the Z components while the green bars represent planimetric residu-

als; there are three green lines, in general, because each CKP is determined three times, in the NB, NF and BF models. The Y residuals increase in size with the distance from the axis of the strip and are positive in the upper half of the strip and negative in the lower one.

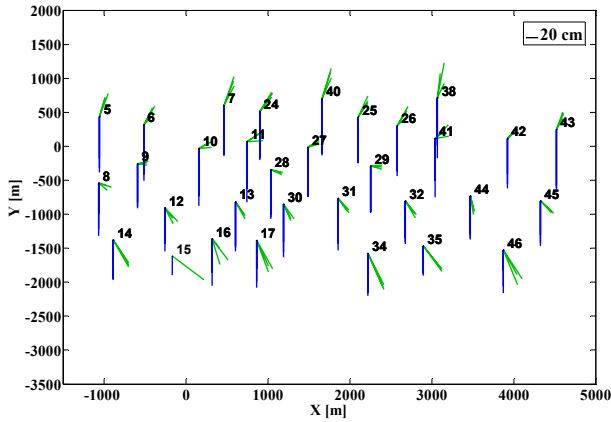


Figure 3. Residuals for along-track models of 0807 strip

The described phenomenon is effectively illustrated by Figure 4 in which each CKP measured is represented by a dot and the three colours used indicate the strip in which measurements were performed. In abscissa the offset of CKPs is indicated with respect to strip axis; in ordinate, the Y residual is shown. The three clouds are not centered around the point having abscissa 0 because of the presence of biases in the residuals, already reported in Table 3. Moreover point distributions clearly show a linear trend indicating that residual size increases with the offset from strip axis, while signs are opposite in the two sides.

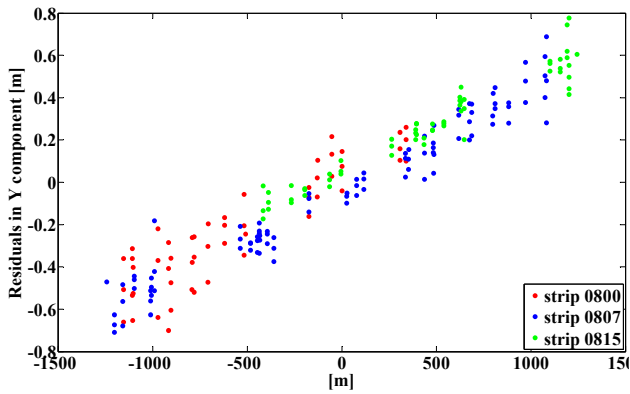


Figure 4. Y residuals as a function of the offset from strip axis

The above mentioned Y bias can also be explained: it is absent in the central strip, named 0807, which is homogeneously covered by CKPs; it is negative for the upper strip, 0800, which is covered by points only in its mid-lower part; finally it is positive for the lower strip 0815, having CKPs in the mid-upper part.

5. NEW CAMERA CALIBRATIONS

Camera self-calibration was performed for the three blocks acquired at the flying heights 2000, 4000 and 6000 m. Before presenting the results, it is worth illustrating some background. The Leica ADS40 camera follows the nominal model briefly illustrated at the beginning of Section 4. As no real camera strictly follows the nominal model, in-flight calibration is per-

formed by the manufacturer and deviations from the theoretical model, caused by lens distortion, offset and inclination of sensor lines, are quantified. A mathematical model of deviations is estimated and then calibration files are written. They contain, for every sensor line, a look-up table with the image coordinates of the centre of each CCD element: these coordinates are determined in order to compensate for any distortion.

The conversion between the pixel coordinates (those originally measured when the user clicks on a image or when an algorithm locates a feature) and the image coordinates of a certain feature is performed through the look-up tables, therefore the obtained image coordinates are virtually free of any distortion and can be inserted into the canonical collinearity equations.

The mathematical model implemented in Orima was defined by Brown (1976): it has 21 parameters and was originally defined for large-format, analogue frame cameras, but it has been successfully applied to line cameras too.

When the camera self-calibration is performed by Orima, the program writes new copies of the above-mentioned look-up tables: calibration files are written to a devoted directory of the hard disk, one for each of the camera's CCD lines. Because of their extension, these files are called CAM files.

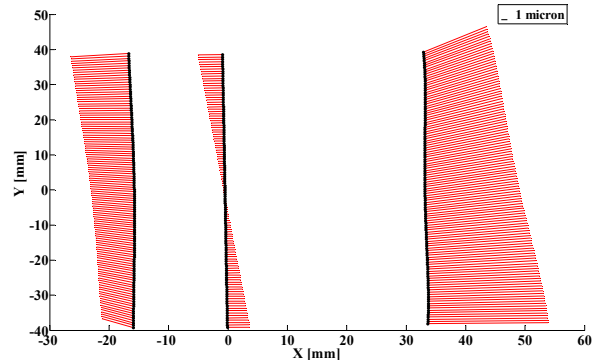


Figure 5. CAM-2000 files compared to the original CAM ones

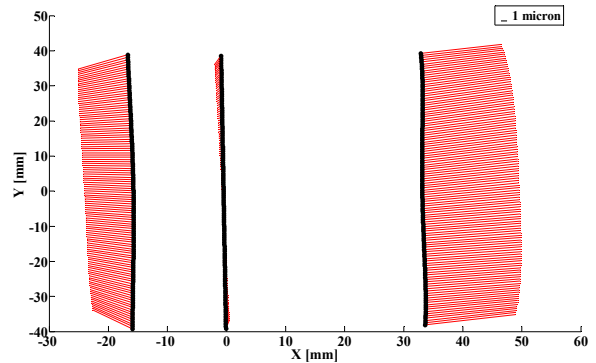


Figure 6. CAM-4000 files compared to the original CAM ones

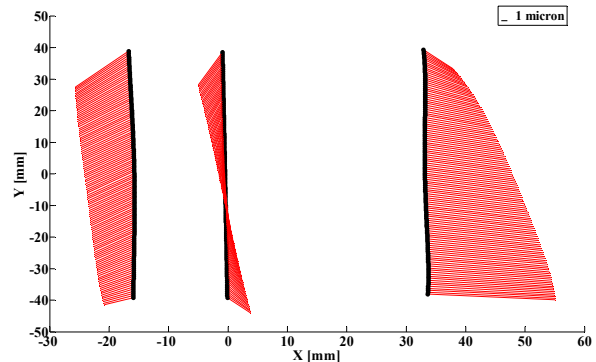


Figure 7. CAM-6000 files compared to the original CAM ones

The company which acquired the dataset supplied us with the imagery and the CAM files created by Leica in March 2004. These original calibration files were used for the experiments described till now. Besides this, camera self-calibration was performed for the three blocks acquired at the flying heights 2000, 4000 and 6000 m, with the Orima software. Consequently three new sets of CAM files were created, denominated CAM-2000, CAM-4000 and CAM-6000 in the following. It is worth noting that the blocks at 2000 m and 6000 m were both acquired on 14.8.2004 while the 4000 m block was acquired 5 days later, on 19.8.2004.

Thanks to specifically written Matlab tools, the four CAM sets were read and analyzed. The new calibrations are compared with the original one in the Figures 5, 6 and 7.

In the Figures, the image coordinates of the CCD elements contained in the original CAM files are shown as black lines; the red lines represent the variations of the newly determined calibration files. These variations are very significant in size, up to 21 microns, roughly corresponding to 3 pixels. Moreover, interestingly, the three new CAM files have roughly the same shape.

6. RE-ASSESSMENT OF THE 2000 M FLIGHT WITH THE NEW CALIBRATIONS

In the previous Section, new camera calibrations are obtained and compared with the original one. In the present section, two topics are investigated:

- the accuracy gain brought by the adoption of the new calibrations;
- the degree of generality of the newly generated CAM files.

To face the first question, the CAM-2000 files are adopted and DG and BASIC scenarios are assessed again. To reach this goal we succeeded in getting Orima read and use the new calibration files, instead of the original ones.

For the sake of homogeneity with Section 3, multiple forward intersection of CKPs is performed.

Set	GCPS/ CKPs	Comp.	Mean [m]	STD [m]	RMSE [m]
DG-2K-2K	0 / 46	x	0.015	0.121	0.122
		y	0.004	0.079	0.080
		z	0.057	0.125	0.138
BASIC-2K-2K	12 / 34	x	-0.017	0.057	0.059
		y	-0.001	0.033	0.033
		z	0.051	0.079	0.094

Table 6. Assessment of the 2000 m flight with the CAM-2000 calibration, in terms of multiple forward intersection

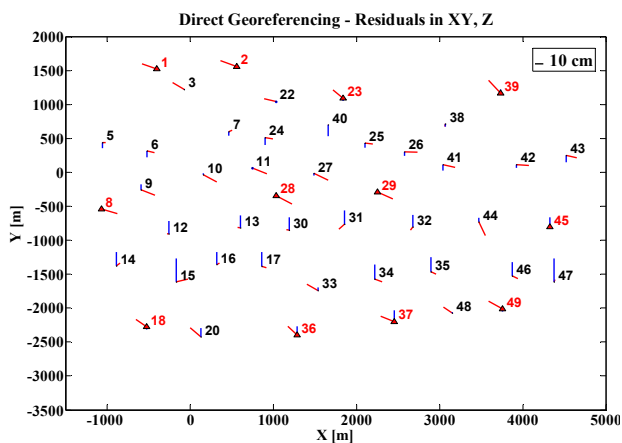


Figure 8. Object space residuals obtained for the DG-2K-2K scenario

Table 6 was obtained with the CAM-2000 calibration and can be compared to Table 1, which was obtained using the original CAM files. Figure 8 shows residuals for direct georeferencing and must be compared to Figure 2. For the sake of clarity, in the following, the names DG-2K, BASIC-2K and SELF-2K will be associated to the experiments performed on the 2000 m block with the original camera calibration, reported in Table 1. When new camera calibrations are used, the assessment scenarios will be denominated with a composite name; for instance BASIC-2K-4K means the assessment of the 2000 m block with the BASIC orientation strategy and with the camera calibration determined with the 4000 m block.

Table 6 reports DG-2K-2K and BASIC-2K-2K. Regarding DG-2K-2K, the Z bias has almost disappeared and RMSE values are all below 70% of the pixel size: it is a very good result. The origin of the Z bias shown in Table 1 is not GPS but camera miscalibration.

BASIC-2K-2K outperforms BASIC-2K and is comparable to SELF-2K. Planimetric RMSE values are below 1/3 of the pixel size and coincide with those of SELF-2K; the Z RMSE is 0.094 m, equal to 45% of GSD, but 1.5 times higher than the corresponding value in SELF-2K. It must also be considered that the SELF-2K scenario also includes a datum transformation determination and IMU misalignment re-estimation, which are not performed in BASIC-2K-2K, being a mere aerial triangulation. In conclusion, the adoption of the new CAM-2000 for the 2000 m block determines a great accuracy improvement.

The question arises now about the significance of the new CAM files. Are they simply the result of a fitting procedure? This would mean that their validity is restricted to the block used to calculate them. Can they be considered a new calibration of the camera, instead? The similarity between the three new calibrations, shown in Figures 5, 6 and 7 seems to confirm the second hypothesis, though partially. We are aware that the methodology used to determine the new calibrations has some limitations, as the blocks used neither have strips re-flown in reverse, nor cross strips. Moreover, Leica usually simultaneously adjust two or three blocks flown at different heights, in order to average some error sources, such as air refraction, while, in the experiments described, only single-block adjustments are performed.

Nevertheless, a first empirical evaluation of significance is performed, assessing the 2000 m block with the calibration determined with the 4000 m block, which was acquired 5 days later than the others.

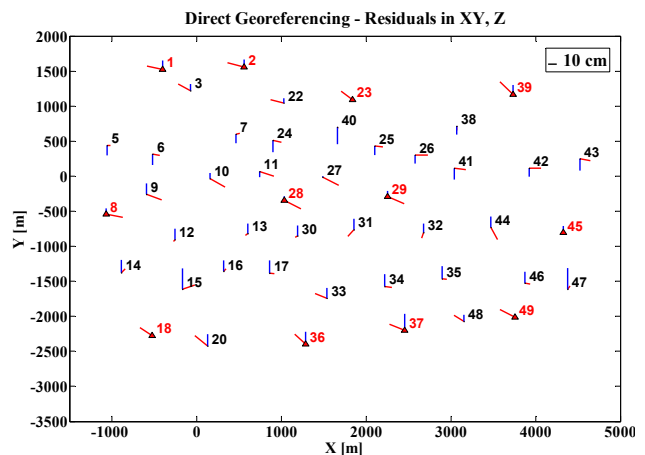


Figure 9. Object space residuals obtained for the DG-2K-4K scenario

Set	GCPs/ CKPs	Comp.	Mean [m]	STD [m]	RMS [m]
DG_2K-4K	0 / 46	x	0.014	0.126	0.126
		y	0.005	0.079	0.080
		z	0.061	0.138	0.150

Table 7. Assessment of the 2000 m flight with the CAM-4000 calibration, in terms of multiple forward intersection

Table 7 and Figure 9 show that the scenarios DG_2K_2K and DG_2K_4K, which are identical in everything but the calibration, perform almost equivalently. The attainable accuracy for the 2000 m block is greatly increased when the new calibrations are used instead of the original ones.

7. CONCLUSIONS

An in-depth analysis of camera systematic errors is performed for the Leica ADS40, with a dataset acquired over the Pavia Test Site in August 2004. The existence of small biases in IMU misalignment -very probable- is not investigated in the paper.

The 2000 m block is initially assessed using the original calibration data, issued on 1.3.2004.

A detailed analysis based on single-model measurements is successively performed for the 2000 m block, highlighting phenomena which are hidden when the usual multiple forward intersection of CKPs is executed. Its main outcome is that, in DG, along-track and across-track models behave very differently, highlighting the existence of camera systematic errors.

Camera self-calibration is then performed, for the three available blocks, having different flying heights. The so-produced calibration files are analyzed and compared between themselves (there is similarity) and to the original ones (there are significant differences).

Finally the new calibrations are adopted and the 2000 m block is assessed again. Accuracy is greatly increased for DG, which now shows very interesting figures, as well as for the BASIC scenario. Experiments highlight that the internal camera geometry significantly changed between March and August 2004; it is also demonstrated that, with the proper calibration file, very good accuracies are attainable without camera self-calibration and even with direct georeferencing.

Further analyses are required to establish a link between the estimated calibration variations and physical quantities and to ascertain whether there is a reasonable time extent over which the geometry of the camera is substantially stable.

The research presented in the paper was carried out within the frame of the National Research Project entitled *Analysis, Comparison and Integration of Digital Images Acquired by Aerial and Satellite Platforms*, co-funded by the Italian Ministry of the University for the year 2005 and chaired by prof. Dequal of the Technical University of Torino.

The Company Compagnia Generale Ripresearee, Parma, Italy is acknowledged for supplying the dataset used.

8. REFERENCES

Brown, D.C., 1976. The Bundle Adjustment – Process and Prospects. Invited Paper to the 13th Congress of the ISPRS Comm. III, Helsinki.

Casella, V., Franzini, M., Kocaman, S., Gruen, A., 2007. Triangulation and Self-calibration of the ADS40 Imagery: A Case

Study over the Pavia Test Site. 8th Conference on “Optical 3D Measurement Techniques”, Zurich, Switzerland, 9-12 July.

Casella, V., Franzini, M., Padova, B., 2007. Accuracy assessment of ADS40 imagery as a function of flying height and of aerial triangulation strategies. Proceedings of 5th MMT Symposium, 29-31 May 2007, Padova, Italy, published on CD).

Casella, V., Franzini, M., Padova, B. (2007). Valutazione dell'accuratezza delle immagini ADS40 in funzione del modello di camera e della quota di volo. Proceedings of the 11th ASITA National Conference, 6-9 November 2007, Torino, Italy.

Cramer, M. (2006). The ADS40 Vaihingen/Enz geometric performance test. *ISPRS Journal of Photogrammetry and Remote Sensing*, Volume60, Issue 6, September 2006, pp. 363-374.

Cramer, M., 2007. The EuroSDR Performance Test for Digital Aerial Camera Systems. Proceedings of the 51st Photogrammetric Week, Stuttgart, Germany. 3-7 September, pp.89-106.

Gruen, A., Zhang, L., 2003. Sensor Modeling for Aerial Triangulation with Three-Line-Scanner (TLS) Imagery. *Journal of Photogrammetrie, Fernerkundung, Geoinformation*, 2/2003, pp. 85-98.

Hinsken, L., Miller, S., Tempelmann, U., Uebbing, R., Walker, S., 2002: Triangulation of LH Systems'ADS40 imagery using ORIMA GPS/IMU. Proceedings of ISPRS Commission III Symposium, on CD. 9-13 September, Graz, Austria.

Kocaman, S., Zhang, L., Gruen, A., 2006: Self-calibrating Triangulation of Airborne Linear Array CCD Cameras. EuroCOW 2006 International Calibration and Orientation Workshop, Castelldefels, Spain, 25-27 Jan. (proceedings on CD-ROM).

Kocaman, S., Casella, V., Franzini, M., Gruen A., 2007. The triangulation accuracy OF ADS40 imagery over the Pavia Test-site. Proceedings of Annual Meeting of U.K. Remote Sensing and Photogrammetry Society 2007, together with the ISPRS Comm. I WG 4 “Airborne Digital Photogrammetric Sensor Systems” Workshop, Newcastle upon Tyne, U.K., 12-17 September (proceedings on CD-ROM).

Kocaman, S., Gruen, A., Casella, V., Franzini, M., 2007. Accuracy assessment of ADS40 imagery over Pavia Testsite. Proceedings of 28th Asian Conference on Remote Sensing (ACRS 2007), November 12-16, 2007, Kuala Lumpur, Malaysia.

Sandau, R., Braunecker, B., Driescher, H., Eckardt, A., Hilbert, S., Hutton, J., Kirchhofer, W., Lithopoulos, E., Reulke, R., Wicki, S., 2000: Design Principle of The LH Systems ADS40 Airborne Digital Sensor. The International Archives of Photogrammetry and Remote Sensing, Amsterdam, Vol. 33, Part B1, pp. 258-265.

Tempelmann, U., Hinsken, L., Recke, U., 2003: ADS40 Calibration and Verification Process. Proceedings of Optical 3D Measurement Techniques Conference, Zurich, Switzerland, pp. 48-54.